Full Text View

Volume 31, Issue 11 (November 2001)

Journal of Physical Oceanography
Article: pp. 3249–3257 | Abstract | PDF (119K)

Production Functions of Film Drops by Bursting Bubbles

Jin Wu

Institute of Hydraulic and Ocean Engineering, National Cheng Kung University, Tainan, Taiwan

(Manuscript received January 28, 2000, in final form April 3, 2001)

DOI: 10.1175/1520-0485(2001)031<3249:PFOFDB>2.0.CO;2

ABSTRACT

Experimental results of Blanchard and Syzdek and of Resch and Afeti on the production of film drops by bubbles bursting at the surface of seawater were parameterized earlier by Wu. More recently, comprehensive observations have been carried out by Spiel. All these measurements, covering different size ranges of film drops, are shown to quantitatively complement each other. Through combining these results, the production of film drops has been quantified, in terms of both number and size distribution, over the entire radius range 0.01–250 μm. The average size of film drops is about 25 μm in radius, which is much larger than the commonly cited radius for film drops of 5 μm. In addition, all the results are shown to follow a simple rule; that is, the ratio between the total surface area of film drops and the surface area of their parent bubble is a constant.

1. Introduction

Marine aerosols have been associated with many environmental phenomena; these include the formation of cloud (Woodcock 1952) and the radiative transfer (Barber and Wu 1997), heat exchange (Andreas 1992), and chemical fractionation (Duce and Hoffman 1976) at the air–sea interface. They are also involved in material corrosion (Ruskin et al. 1981) and light extinction (Schacher et al. 1981) within the marine atmosphere and a feedback mechanism for global warming (Latham and Smith 1990). Droplets of marine origin have been considered to be produced substantially by air bubbles bursting at the sea surface (Blanchard 1963; Wu 1981); these bubbles are formed by air entrained into the near-surface ocean by breaking waves (Wu 1994a). Droplets produced through the fragmentation of bubble film cap are film drops (Blanchard 1963; Day 1964), and those produced through the breakup of a water jet formed by the collapse of bubble cavity are jet drops (Kientzler et al. 1954). The production of jet drops by bubbles of various sizes was quantified first (Kientzler et al. 1954), while observations on the production of film drops took place much later (Resch et al. 1986; Blanchard and Syzdek 1988; Resch and Afeti 1991;

Resch and Afeti 1992). Wu (1994b) showed that numbers of film drops observed in these investigations over various size ranges followed a common power law: the number of film drops produced increased with the square of bubble radius. In addition, size spectra of large film drops (>45 μm in radius) produced by bubbles of different radii were found to be nearly universal; the remaining spectrum of smaller drops was then deduced from productions measured over various size ranges.

More recently, comprehensive observations on film drops were carried out by Spiel (1998), especially for large sizes. The average radius of film drops in his measurements is shown to increase with the bubble radius. Spiel's results are herewith combined with those reported earlier (Blanchard and Syzdek 1988; Resch and Afeti 1991) to develop further the size spectrum, and to deduce the numerical production function, of film drops covering the entire radius range of 0.01–250 μm. All size distributions are shown to follow a general spectrum refined from that suggested earlier (Wu 1994b); the sizes of film drops are larger than previously recognized. The number of film drops produced was found to be proportional with the surface area of their parent bubble; the total surface area of film drops is, therefore, a constant fraction of the surface area of their parent bubble.

2. Earlier results

a. Total number

The bursting of artificially produced bubbles at the surface of seawater was observed by Resch et al. (1986) with a laser holographic technique. Numbers were reported for film drops produced by four single bubbles having radii of 1, 2, 3, and 4 mm. Subsequently, bubbles over a similar size range were steadily generated by Blanchard and Syzdek (1988), by forcing nucleus-free air through a capillary tip in seawater. Upon bursting of generated bubbles at the water surface, film and jet drops were ejected into a slow stream of filtered air, which carried only small drops, presumably film drops, with their radii smaller than 4 μm through a condensation nucleus counter. Blanchard and Syzdek stated that the counter could detect drops as small as 0.015 μm in radius with an efficiency of 100%, but down to about 10% at 0.0025 μm; Wu (1994a) rounded off the lower bound of their detection as 0.01 μm in radius. These developed techniques of producing bubbles and transfering film drops to a counter were later adopted by Resch and Afeti (1991). As for the size measurement, they used an optical counter with a resolution down to 0.4 μm in radius to cover the range 0.4–20 μm, and adopted the laser holographic technique of Resch et al. to cover 20–250 μm. Measurements were performed with 8–16 bubbles of each radius, instead of only a single one as in the earlier study (Resch et al. 1986).

Power laws were first suggested by Wu (1989) and used later by Resch and Afeti (1991) to represent the number of film drops produced in earlier sets of data (Blanchard and Syzdek 1988; Resch et al. 1986; Resch and Afeti 1991) shown in Fig. 1a

$$N = aR^n, \quad (1)$$

where N is the total number of film drops produced by a bubble having radius R expressed in millimeters. It should be noted that a “strong peak” (those two data points marked with question marks in Fig. 1a) was reported by Blanchard and Syzdek (1988). This peak was further narrowed by Resch and Afeti (1992) to occur right at the bubble radius of 1.07 mm, but the mechanism of its production was still unexplained. Further studies of this interesting phenomenon are definitely needed, at this stage, we are unable to include this “singular event” in our analyses.

Power laws that result from fitting Eq. (1), on the basis of orthogonal least squares, to each of the datasets shown in Fig. 1a, are reproduced from Wu (1994b) in Table 1. In this first round of curve fitting, both the coefficient a and exponent c were allowed to vary. Values of the exponent are seen in the table to range narrowly between 1.97 and 2.08, having an average value of about 2. A second round of curve fitting was then performed to find the coefficient b of the power law $N \sim bR^2$ (see the bottom row in Table 1).

As mentioned earlier, film drops are produced by fragmentation of a bubble film cap, the area of which is proportional to the square of bubble radius. The numerical production of film drops should therefore be governed by the surface area of bubble cap, provided that size spectra of film drops produced by bubbles having various radii are nearly universal. Such a size spectrum has been shown earlier (Wu 1994b) and will be further verified to exist. In other words, the numerical production of film drops being proportional to the square of bubble radius, $N \propto R^2$, was discussed to be entirely consistent with the concept that these drops are produced by the bursting of bubble film cap.

b. Size spectrum

Size distributions of film drops produced by bursting bubbles were also obtained by Resch and Afeti (1991). The probability of occurrence, $f(r)$, was reported for each radius band, where r is the radius of film drop. Results are reproduced from Wu (1994b) in Fig. 1b. First of all, the data obtained from bubbles of various radii were suggested to have nearly a

universal size spectrum on the large radius side. A line corresponding to

$$f(r) \sim r^{-2}, \qquad r > 45\ \mu\text{m} \quad (2)$$

was fitted to the data as Line 1 in Fig. 1b. Accepting the production function $N = bR^2$ and values of the coefficient b shown in Table 1, Wu reasoned that the spectral density from 45 μm toward smaller radii could neither remain constant nor decrease monotonically. Through the matching of drop populations measured by Blanchard and Syzdek (1988) and Resch and Afeti (1991) over different but overlapping size ranges, the size spectrum for small drops was shown to follow:

$$f(r) \sim r^{-1/2}, \qquad r < 45\ \mu\text{m}. \quad (3)$$

This is represented by Line 3 in Fig. 1b. This will be discussed further in a later section.

In summary, Line 1 in Fig. 1b, representing the nearly universal size spectrum at large radii, is believed to be accurately determined from data provided by Resch and Afeti (1991). Smaller drops obtained from the same set of data and represented by Line 2, on the other hand, were suggested to be undercounted. Line 3 was determined by taking into account not only the entire set of data from Resch and Afeti, but also that from Blanchard and Syzdek (1988); the latter was especially reliable at small radii.

3. Extended results

a. Recent observations

Detailed processes on the birth of film drops from bubbles bursting at the surface of seawater were recently observed by Spiel (1998). Results were obtained with bubbles of eight different radii in the range of 1.47–6.29 mm. An optical probe consisting of a laser and a linear array of photodiodes was used to measure film drops over the radius range of 5–300 μm. For each size of bubbles, numbers of film drops per burst over various size bands were reported; results are reproduced in Fig. 2, in which the data are seen to actually start at the radius of 9 μm and not to extend beyond 250 μm.

The total number of film drops per bursting obtained from data presented in Fig. 2 is shown in Fig. 3. Spiel (1998) also proposed a linear relationship to describe his results, with the total number increasing linearly with the bubble radius.

b. Further analyses

1) TOTAL NUMBER

Size ranges of bubbles tested and those of film drops measured in different studies are summarized in Table 2.

From the results presented in Table 1, the total number of film drops observed by Resch and Afeti (1991) over the entire radius range of 0.4–250 μm of their measurements can be represented from Table 2 as $3.81R^2$; the latter is the sum of productions from radius ranges of 0.4–20 and 20–250 μm. This is shown as a solid line in Fig. 3, along with that for the radius range of 20–250 μm as a dashed line; results of Blanchard and Syzdek (1988) are presented as a dotted line. It is, of course, nice to see in the figure that most total numbers obtained by Spiel (1998) for the size range 9–250 μm are below the solid line covering a wider range (0.4–250 μm) and above the dotted line covering a narrower range (20–250 μm). Only two of the data points appear not to fit this description. Of these two, the production with the smallest bubble is indeed seen to be quite low. It was probably due to the resolution of Spiel's technique in measuring small drops and the nature of results. As illustrated in Figs. 2 and 3, a missed count of a single film drop with small bubbles would drastically alter the results. Judging from power laws established from other investigations shown in Fig. 1a and the consistent trend displayed by a great majority of Spiel's data points, we accept again the R^2 power law. A dashed and dotted line was then fitted to Spiel's data, which can be written as

$$N = 2.85R^2, \quad (4)$$

in which the bubble radius R is again expressed in millimeters, and the coefficient in the above expression is also shown in Table 2.

2) SIZE SPECTRUM

Size spectra of film drops observed by Spiel (1998) are reproduced, from his data shown in Fig. 2, in Fig. 4a. Data from various sizes of bubbles appear to follow the same pattern but are spread out, making it difficult to detect their

trends. We then attempted the following normalization.

From Spiel's (1998) data shown in Fig. 2, we obtained first the average radius of film drops; see the bottom frame in the figure. Note that the average radius in this case was calculated strictly from his measurements over the radius range 9–250 μm. For a determination of the true average radius, we need to have a complete size distribution to cover all radii. From the size distributions shown in Fig. 2, it is apparent that not all of them are peaked; moreover, as shown in Fig. 4 there are many more drops at radii smaller than 9 μm. The average radius of Spiel's measurements is seen in Fig. 2 to increase with the bubble size, following quite closely a linear variation shown in the figure, or

$$\bar{r} = 10 + 6.5R, \quad (5)$$

in which $\bar{r}$ is the average drop radius expressed in μm, and R is still in mm.

With average radii shown in Eq. (5), we normalized size spectra of film drops obtained by Spiel (1998) from bubbles of various radii (see Fig. 4b). Trends now become more clear. As discussed earlier, Spiel's data obtained with bubbles having the smallest radii may not be as accurate as those at larger radii. All datasets except those two associated with smallest bubbles are clustered together; they are also seen to peak at $r/\bar{r} = 0.7$. Two straight lines are drawn in the figure to illustrate that the data follow well a r^{-2} dropoff up to $r/\bar{r} = 2.5$; then, the dropoff becomes more rapid, following r^{-4}. Trends are not clear for drops on the small radius side of the peak; this portion is also beyond the bulk of Spiel's measurements.

Now, let us refer trends discussed above to data shown in Fig. 4a. We see that the data appear to peak at $r = 30$ μm, follow the r^{-2} dropoff until $r = 100$ μm, and the r^{-4} dropoff over larger sizes. We also believe that Spiel's (1998) data are not only more comprehensive but also more accurate than those of Resch and Afeti (1991) for drops larger than 30 μm shown on the large radius side of the peak in Figs. 4a,b. The size spectrum on the large-radius side is, therefore, modified as

$$\begin{aligned} f(r) &\sim r^{-2}, \qquad 30\ \mu\text{m} < r \leq 100\ \mu\text{m} \\ f(r) &\sim r^{-4}, \qquad r > 100\ \mu\text{m}. \end{aligned} \quad (6)$$

As discussed earlier, we need other measurements over small radii, say below 30 μm in radius, first to deduce the shape of spectrum and then to enable us to describe it quantitatively. Measurements of film drops produced by simulated breaking waves were reported by Cipriano and Blanchard (1981) and Woolf et al. (1987); their results indicated clearly the importance of extending the spectrum to small drops.

4. Further quantifications

a. Initial quantification

The radius range of film drops is quite likely to cover 0.01–250 μm. Resch and Afeti's (1991) measurements actually had two parts, covering, respectively, radius ranges of 0.4–20 μm and 20–250 μm. We can then subtract the latter portion from Spiel's (1998) data covering 9–250 μm to obtain the production for the range 9–20 μm. The difference between Resch and Afeti's total coverage 0.4–250 μm and Spiel's represents the production for the radius range 0.4–9 μm. All these portions of the production along with Blanchard and Syzdek's (1988) measurements covering 0.01–4 μm are summarized in Table 3. Still the portion over the small-radius end of 0.01–0.4 μm is missing; hence we cannot obtain directly from these partial productions the total population for the entire radius range 0.01–250 μm.

Judging from the spectral shape discussed in the previous section, as in Wu (1994b) we now attempt to approximate the total production spectrum of film drops with

$$\begin{aligned} f(r) &\sim r^{m}, \qquad r \leq 30\ \mu\text{m} \\ f(r) &\sim r^{-2}, \qquad 30\ \mu\text{m} < r \leq 100\ \mu\text{m} \\ f(r) &\sim r^{-4}, \qquad r > 100\ \mu\text{m}. \end{aligned} \quad (7)$$

The above spectrum is diagramed in Fig. 5a in arbitrary scales, along with radius ranges of various measurements. We then integrate this spectrum over those radius ranges shown in the figure for the purpose of evaluating the production coefficient b in

$$N = bR^2. \quad (8)$$

Spiel's (1998) measurement is considered to be more accurate, and therefore is adopted as the basis for comparison. For various values of the exponent m, ratios between areas over first three radius ranges shown in Table 3 and that over the fourth (base) range were first obtained. These areas, of course, indicate relative productions of film drops; they were then compared with measurements indicated by the coefficient b shown in the last column of Table 2. For exact matches with Spiel's results, values of m should be −0.61 for Blanchard and Syzdek's (1988) measurements over the radius range 0.01–4 μm, −0.24 for Resch and Afeti's (1991) over the range 0.4–20 μm, and 0.03 over the range 20–250 μm. In other words, the uncertainty in the spectrum for the small-radius side is between $r^{0.03}$ and $r^{-0.61}$. First of all, the data may not warrant the identification of an exponent to two significant figures, such as −0.61. Therefore, it was decided to test candidate exponents of 0, −1/4, −1/2, and −3/4.

As mentioned earlier, the purpose of this portion of the exercise is not only for completing the size spectrum, but also for deducing the total production of film drops. The results of attempting the latter, as illustrated earlier, could not be obtained by simply summing up production rates over various size ranges. We need to synthesize those production rates for overlapping size ranges with the size spectrum. For each of four exponents tentatively chosen above, we determined first the ratio between the area under the spectrum for a particular radius range of measurements and that for the entire range 0.01–250 μm. Then, the total production rate was obtained from the partial rate over this particular range, by dividing it with the area ratio just determined. Results are presented in Table 4, in which b_1, b_2, b_3, and b_4 are assigned to represent the production rates determined from respectively four radius (μm) ranges 0.01–4 (Blanchard and Syzdek 1988), 0.4–20 and 20–250 (Resch and Afeti 1991), and 9–250 (Spiel 1998).

As expected, the choice of exponent m is quite sensitive to results obtained from small radius ranges. For m = −1/2, all production rates appear to be reasonably close to their average value of b = 4.0. The choice of m = −1/4 produced the closest results across the last three size ranges. We need, however, to exclude that for the first range in the average; in this case, the average value is 3.86, which is quite close to the value of 4.0 just obtained. Our attempt as discussed earlier is two fold, to obtain from measurements over four radius ranges the complete size spectrum, and to obtain the total production rate of film drops. Between m = −1/2 and −1/4 we see that the former appears to be the best choice as it not only provides an average value matching the most likely value of 4.0, but also results in the least scatter among the b coefficients. Results obtained with m = −3/4 and 0 are then clearly not to be the choice, for exactly those reasons discussed above. We finally have

$$b = 4.0 \quad \text{and} \quad m = -1/2. \tag{9}$$

The exponent actually is the same as that obtained earlier with only data of Blanchard and Syzdek (1988) and of Resch and Afeit (1991), but the portion of spectrum, $r^{-1/2}$, is over a different radius range.

b. Final quantification

With the selection of m = −1/2, we can now determine the true size spectrum; see Fig. 5b, in which the area under the spectrum over the radius range 0.01–250 μm is unity. The probability density of occurrence, $p(r)$, for the film drop having radius r, expressed in μm, can be found as

$$\begin{aligned} p(r) &= 0.066r^{-1/2}, && 0.01\ \mu\text{m} < r \le 30\ \mu\text{m} \\ p(r) &= 10.9r^{-2}, && 30\ \mu\text{m} < r \le 100\ \mu\text{m} \\ p(r) &= 1.09 \times 10^5 r^{-4}, && 100\ \mu\text{m} < r < 250\ \mu\text{m}. \end{aligned} \tag{10}$$

The number of film drops per μm radius increment, $n(r)$, centered on the radius r produced by the bursting of a bubble having radius R at the surface of seawater therefore follows:

$$n(r) = Np(r), \qquad N = 4R^2. \tag{11}$$

Finally, we can now calculate the average radius for the entire size range 0.01–250 μm to be 24.9 μm.

The above quantification synthesized results of Blanchard and Syzdek (1988), Resch and Afeti (1991), and Spiel (1998). As mentioned earlier, observations of film drops were also performed by Cipriano and Blanchard (1981) and Woolf et al. (1987); drops in these studies, however, were produced by bubbles of various sizes in a simulated breaker, not from individual bubbles of a given size. Most film drops were reported to be small than 5 μm in the former study and 2 μm in the

latter. Similarly, Andreas (1998) indicated that film drops were most plentiful for the radius range 0.5–5 μm. Although all of these are not the average radius indicated in the previous paragraph, we still see that film drops are perhaps somewhat larger than commonly conceived.

5. Physical parameterization

The production of film drops is obviously governed by the surface area of their parent bubble. This is actually suggested by the results that the number of film drops produced increases with the bubble radius, following R^2; the latter is, of course, proportional to the bubble surface area. There are three variables involved in this phenomenon: the number and radius of film drops produced and the radius of bubble. Among them there is only one basic dimension involved: the length. According to the π theorem of dimensional analysis, only one nondimensional parameter can be formed, and this parameter should have a constant value. Physically, the surface area, which is the square of length scale, is important; an obvious nondimensional parameter is therefore

$$\bar{r}^2_a/R^2 = \text{const} \quad (12)$$

in which $\bar{r}_a$ is the spectrally weighted average of film drop radius. The total surface area of film drops can be obtained from

$$S_f = N \int_{r_1}^{r_2} 4\pi r^2 p(r)\, dr,$$

$$r_1 = 0.01 \quad \text{and} \quad r_2 = 250\ \mu\text{m} \quad (13)$$

in which S_f is the total surface area of film drops and N is given in Eq. (11). Then the ratio between total surface areas of film drops and bubbles is

$$I = S_f/4\pi R^2 = 6.19 \times 10^{-3}. \quad (14)$$

In other words, only a very small fraction of the film cap of bubble is used to produce film drops. Accordingly, as suggested by one of the referees, the bubble appears to ride very low in water when it bursts. He further indicated that this was not incompatible with photographs of Kientzler et al. (1954).

6. Concluding remarks

Measurements of film drops produced by individual bubbles bursting at the surface of sea water by Blanchard and Syzdek (1988), Resch and Afeti (1991), and Spiel (1998) over four different but overlapping size ranges are shown to be remarkably consistent. Taken together, we obtained the complete size spectrum and the total production rate over the entire radius range 0.01–250 μm. The size of film drops was found to be several times greater than commonly considered. The power law describing the production rate can be deduced from the dimensional analysis. The total surface area of film drops is less than 1% of that of their parent bubble.

Acknowledgments

I am very grateful for comments of both referees. This work was supported by the National Science Council under Grant NSC88-NSPO(A)-PC-FA09-02.

REFERENCES

Andreas E. L, 1992: Sea spray and the turbulent air–sea heat fluxes. *J. Geophys. Res*, **97**, 11429–11441. Find this article online

Andreas E. L, 1998: A new sea spray generation function for wind speed up to 32 m s^{-1}. *J. Phys. Oceanogr*, **28**, 2175–2184. Find this article online

Barber R. P., and J. Wu, 1997: Sea brightness temperature and effects of spray and whitecap. *J. Geophys. Res*, **102**, 5823–5827. Find this article online

Blanchard D. C., 1963: The electrification of the atmosphere by particles from bubbles in the sea. *Progress in Oceanography*, Vol. 1, Pergamon, 71–102.

Blanchard D. C., and L. D. Syzdek, 1988: Film drop production as a function of bubble size. *J. Geophys. Res*, **93**, 3649–3654. Find this article online

Cipriano R. J., and D. C. Blanchard, 1981: Bubble and aerosol spectra produced by a laboratory "breaking wave.". *J. Geophys. Res*, **86**, 8085–8092. Find this article online

Day J. A., 1964: Production of droplets and salt nuclei by the bursting of air bubble films. *Quart. J. Roy. Meteor. Soc*, **90**, 72–78. Find this article online

Duce R. A., and E. J. Hoffman, 1976: Chemical fractionation at the air/sea interface. *Annu. Rev. Earth Planet. Sci*, **4**, 187–228. Find this article online

Kientzler C. F., A. B. Arons, D. C. Blanchard, and A. H. Woodcock, 1954: Investigation of the projection of droplets by bubbles bursting at a water surface. *Tellus*, **6**, 1–7. Find this article online

Latham J., and M. H. Smith, 1990: Effect on global warming of wind-dependent aerosol generation at the ocean surface. *Nature*, **347**, 372–373. Find this article online

Resch F., and G. M. Afeti, 1991: Film drop distributions from bubbles bursting in sea water. *J. Geophys. Res*, **96**, 10681–10688. Find this article online

Resch F., and G. M. Afeti, 1992: Submicron film drop production by bubbles in seawater. *J. Geophys. Res*, **97**, 3679–3683. Find this article online

Resch F., S. J. Darrozes, and G. M. Afeti, 1986: Marine liquid aerosol production from bursting of air bubbles. *J. Geophys. Res*, **91**, 1019–1029. Find this article online

Ruskin R. E., F. K. Lepple, and K. K. Jeck, 1981: Salt aerosol survey at gas turbine inlet aboard USS *Spruance*. Naval Research Laboratory Memo. Rep. 4419.

Schacher G. E., K. L. Davidson, C. W. Fairall, and D. E. Spiel, 1981:: Calculation of optical extinction from aerosol spectral data. *Appl. Opt*, **20**, 3951–3957. Find this article online

Spiel D. E., 1998: On the births of film drops from bubbles bursting on seawater surfaces. *J. Geophys. Res*, **103**, 24907–24918. Find this article online

Woodcock A. H., 1952: Atmospheric salt particles and raindrops. *J. Meteor*, **9**, 200–212. Find this article online

Woolf D. K., P. A. Bowyer, and E. C. Monahan, 1987: Discriminating between the film drops and jet drops produced by a simulated whitecap. *J. Geophys. Res*, **92**, 5142–5150. Find this article online

Wu J., 1981: Evidence of sea spray produced by bursting bubbles. *Science*, **212**, 324–326. Find this article online

Wu J., 1989: Contributions of film and jet drops to marine aerosols produced at the sea surface. *Tellus*, **41B**, 469–473. Find this article online

Wu J., 1994a: Bubbles in the near-surface ocean: Their various structures. *J. Phys. Oceanogr*, **24**, 1955–1965. Find this article online

Wu J., 1994b: Film drops produced by air bubbles bursting at the surface of sea water. *J. Geophys. Res*, **99**, 16403–16407. Find this article online

Tables

TABLE 1. Coefficients and exponents of power laws, $N = aR^c$ or $N = bR^2$, for various radius ranges. This table is reproduced from Wu (1994b)

b	1.96	1.65	2.16

Click on thumbnail for full-sized image.

TABLE 2. Radius ranges of bubbles tested and film drops measured (coefficient b of $N = bR^2$)

Investigation	Bubble (mm)	Film drop (μm)	Coefficient b
		0.01–4.0	1.96
Blanchard and Syzdek (1988)	0.71–3.14	0.4–20	1.65
Resch and Afeti (1991)	0.52–5.0	20–250	2.16
Spiel (1998)	1.47–6.29	9.0–250	2.85

Click on thumbnail for full-sized image.

TABLE 3. Productions over various radius ranges

Radius range (μm)	0.01–4	0.4–9	9–20	20–250
Coefficient b	1.96	0.96	0.69	2.16

Click on thumbnail for full-sized image.

TABLE 4. Production coefficients determined over various radius ranges

	Coefficients			
Exponent m	b_1	b_2	b_3	b_4
−3/4	2.22	2.22	3.89	3.30
−1/2	6.00	2.50	3.95	3.56
−1/4	14.30	3.76	4.01	3.81
0	31.29	5.36	4.07	4.05
Radius range (μm)	0.01–4	0.4–20	20–250	9–250

Click on thumbnail for full-sized image.

Figures

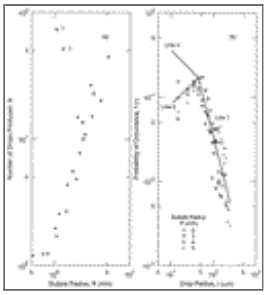

Click on thumbnail for full-sized image.

FIG. 1. Numbers and size spectra of film drops produced by bursting bubbles. These earlier results are reproduced from Wu (1994b). Data in (a) are from Blanchard and Syzdek (1988) (circles) and Resch and Afeti (1991) (measured over two size ranges, pluses: 0.4–20 μm in radius; crosses: 20–250 μm. Data in (b) are from Resch and Afeti. Question marks in (a) and Lines 1, 2, and 3 in (b) are explained in the text

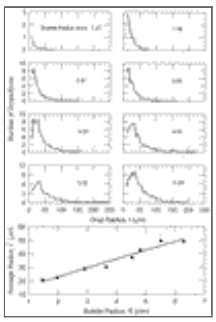

Click on thumbnail for full-sized image.

FIG. 2. Size distributions and average radii of film drops observed by Spiel (1998)

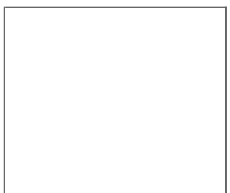

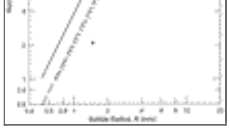

Click on thumbnail for full-sized image.

FIG. 3. Numbers of film drops produced by bubbles of various radii. The results of Resch and Afeti (1991) are represented by two lines (dashed line for 20–250 μm in radius, and solid line for 0.4–250 μm), those by Blanchard and Syzdek (1988) are represented by dotted line for 0.01–4 μm, and the data reported by Spiel (1998) (+ for 9–250 μm and the dashed and dotted line)

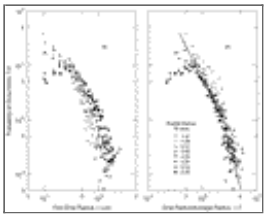

Click on thumbnail for full-sized image.

FIG. 4. Spectra of film drops produced by bursting bubbles: Original (a) and normalized with average radius (b). The data are from Spiel (1998)

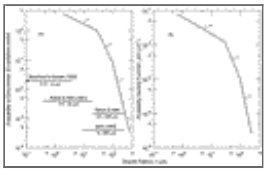

Click on thumbnail for full-sized image.

FIG. 5. Synthesis of various datasets and size specrum of film drops

Corresponding author address: Dr. Jin Wu, Institute of Hydraulic and Ocean Engineering, National Cheng Kung University, Tainan, Taiwan. E-mail: jinwu@mail.ncku.edu.tw

top